

# Arctic sea ice variability during the Instrumental Era

M. Kathleen Brennan, Gregory J. Hakim, and Edward  
Blanchard-Wrigglesworth

<sup>1</sup>Department of Atmospheric Sciences, University of Washington

## Key Points:

- Data assimilation is a skillful technique for reconstructing Arctic sea-ice extent during the satellite era.
- Reconstructed sea ice shows large decline in total Arctic sea-ice extent during the early 20th-century warming (1910–1940).
- Trends in total Arctic sea-ice extent during the satellite era are  $\sim 33\text{--}38\%$  greater than during the early 20th-century warming.

## Abstract

Arctic sea-ice extent (SIE) has declined drastically in recent decades, yet its evolution prior to the satellite era is highly uncertain. Studies using SIE observations find little variability prior to the 1970s; however, these reconstructions are based on limited data, especially prior to the 1950s. We use ensemble Kalman filter data assimilation of surface air temperature observations with Last Millennium climate model simulations to create a fully gridded Arctic sea-ice concentration reconstruction from 1850–2018, and investigate the evolution of Arctic SIE during this period. We find a decline of  $\sim 1.25 \times 10^6$  km<sup>2</sup> during the early 20th-century warming (1910–1940). The 25-year trends during this period are  $\sim 33$ – $38\%$  smaller than the satellite era (1979–2018) but almost twice as large as previous estimates. Additionally we find that variability of SIE on decadal timescales prior to satellite era is  $\sim 40\%$  greater than previously estimated.

## Plain Language Summary

Arctic sea ice is an important part of the climate system, serving as the interface between the ocean–atmosphere system. Arctic sea ice has undergone rapid declines in recent decades, prompting the question of whether there have been changes of similar magnitude in the past. To answer such questions, a long record of sea ice is necessary, but spatially and temporally complete satellite observations are only available starting in 1979. Previous studies combining sea ice observations from various sources during the Instrumental Era (1850–2014) found little variability in sea-ice extent prior to the satellite era, but data availability is limited prior to the 1950s. Here we create an independent estimate of Arctic sea ice from 1850–2018 using a data assimilation approach that blends more abundant temperature observations with data from climate models. Our results show substantial loss of sea ice between 1910–1940, with a rate that is about  $\sim 33$ – $38\%$  less than what has been observed in satellite observations. These results reinforce previous findings that the current trend is unprecedented in duration since 1850, but also that sea-ice variability prior to 1979 is  $\sim 40\%$  larger than previously estimated.

## 1 Introduction

Arctic sea ice is one of the most rapidly changing components of the climate system, affecting surface albedo and modulating ocean–atmosphere interaction through surface fluxes. Large declines in sea ice can impact local ecosystems, human communities, and the global climate system (Meier et al., 2014). Documenting and understanding decadal–centennial variability in sea ice is limited by the availability of high-quality observations, which are only spatially and temporally complete during the satellite era (1978–present) (Fetterer et al., 2017). Furthermore, given the presence of strong radiative forcing during this period, it is difficult to partition the relative role of natural variability (e.g. Ding et al. (2017); England et al. (2019)) and radiative forcing (Notz & Marotzke, 2012) on the rapid Arctic sea ice declines observed in the satellite record. In order to estimate the natural variability of sea ice, a longer record is needed. Here we introduce a novel method to reconstruct sea ice cover from 1850–present, using data assimilation (DA), numerical model data, and observations of surface air temperature (SAT).

The longest Arctic sea-ice extent (SIE) observation-based reconstruction combines various sea ice observation types, ranging from satellite data to shipping records, to extend Arctic sea ice records back to 1850 (Walsh et al., 2017). The Walsh et al. (2017) reconstruction shows little SIE variability before 1970, particularly on decadal to multi-decadal timescales. However, the fidelity of this dataset is limited by gaps in observation availability, particularly before 1953 and during winter months (see below and Supporting Information Figure S1).

60 Although direct observations of sea ice are limited in space and time, instrumen-  
 61 tal observations of SAT are much more abundant. Polar, hemispheric and global mean  
 62 SAT, both in observations and climate models, are known to be tightly coupled to sea  
 63 ice variability on annual and longer timescales (e.g. Gregory et al. (2002); Armour et al.  
 64 (2011); Mahlstein and Knutti (2012); Olonscheck et al. (2019)). Observations show that  
 65 global-mean SAT was relatively stable between 1850–1900 (Morice et al., 2012), which  
 66 may explain low decadal sea ice variability in the Walsh et al. (2017) record. However,  
 67 during the early 20th century (1900–1940), an anomalous warming event is well docu-  
 68 mented across Northern Hemisphere high latitudes (e.g. Hegerl et al. (2018)). The mag-  
 69 nitude of this early 20th century warming (ETCW) was largest during winter months  
 70 (Semenov, 2007; Overland et al., 2004) and similar in spatial structure to that observed  
 71 in the late 20th century.

72 Interestingly, the Walsh et al. (2017) record of Arctic SIE shows much less decline  
 73 during the ETCW than during the satellite record, with one period of decline of  $\sim 0.5$   
 74  $\times 10^6 \text{ km}^2$  between 1920–1945 followed by a recovery of  $\sim 0.5 \times 10^6 \text{ km}^2$  between 1945–  
 75 1950 (see below). The peak loss in Walsh et al. (2017) also lags the period of largest ETCW  
 76 temperature anomalies seen in observations, which together with the modest decline in  
 77 SIE suggests a weak relationship between temperature and sea ice during the ETCW.  
 78 In this paper we investigate the relationship between temperature and sea ice during the  
 79 Instrumental Era using satellite observations, reanalysis, and the Walsh et al. (2017) re-  
 80 construction. Then we use a DA framework to construct a new independent Arctic sea  
 81 ice reconstruction using more abundant SAT observations. We then explore the decline  
 82 of sea ice during the ETCW, and compare the ETCW decline to that observed and re-  
 83 constructed in the satellite era.

## 84 2 Temperature and sea ice in the Instrumental Era

85 We begin by analyzing the relationship between Arctic SAT derived from the Had-  
 86 CRUT4.6.0.0 dataset (HadCRUT, Morice et al. (2012)) and SIE from Walsh et al. (2017).  
 87 We partition the analysis in two ways: by season (April–August and September–March)  
 88 and by time period (pre- and post-1953 for Walsh et al. (2017), plus the satellite era (1979–  
 89 2017)), in order to investigate the effect of observation availability on the Walsh et al.  
 90 (2017) record. We find that the relationship between SAT and SIE from the Walsh et  
 91 al. (2017) and satellite observations generally agree from 1953–present, but differ greatly  
 92 before 1953 (Figure 1).

93 Figure 1 shows that the relationship between SAT and SIE is linear in the satel-  
 94 lite record in both seasons, with  $R^2=0.76$  (September–March) and 0.85 (April–August).  
 95 The Walsh et al. (2017) record also shows a linear relationship for both seasons between  
 96 1953–2013, with a similar slope during winter (Figure 1b) and a slightly steeper slope  
 97 during summer (Figure 1a), both not statistically different from the slope determined  
 98 with satellite observations at the 95% confidence level. In contrast, the earlier part of  
 99 the Walsh et al. (2017) record, between 1850–1952, exhibits a much lower SIE–SAT sen-  
 100 sitivity in summer relative to the satellite era (Figure 1a) and almost no SIE–SAT sen-  
 101 sitivity in winter (Figure 1b). Since SAT is a primary driver of sea ice variability (Olonscheck  
 102 et al., 2019), the inconsistent relationship between these two time periods in the Walsh  
 103 et al. (2017) record suggests either a strong nonlinearity in this relationship during the  
 104 ETCW, or that the reconstruction underestimates SIE–SAT sensitivity.

105 There are at least two possible hypothesis for the reduced sensitivity of SIE–SAT  
 106 in Walsh et al. (2017) before 1953. Firstly, the sensitivity of sea ice to temperature may  
 107 be mean-state dependent, such that in colder, thicker, sea-ice regimes (which may have  
 108 existed in the Arctic during the late 19th and early 20th century) sea ice may be less sen-  
 109 sitive to changes in temperature. However, model simulations of sea-ice sensitivity to tem-  
 110 perature for different mean states (Armour et al., 2011; Mahlstein & Knutti, 2012) do

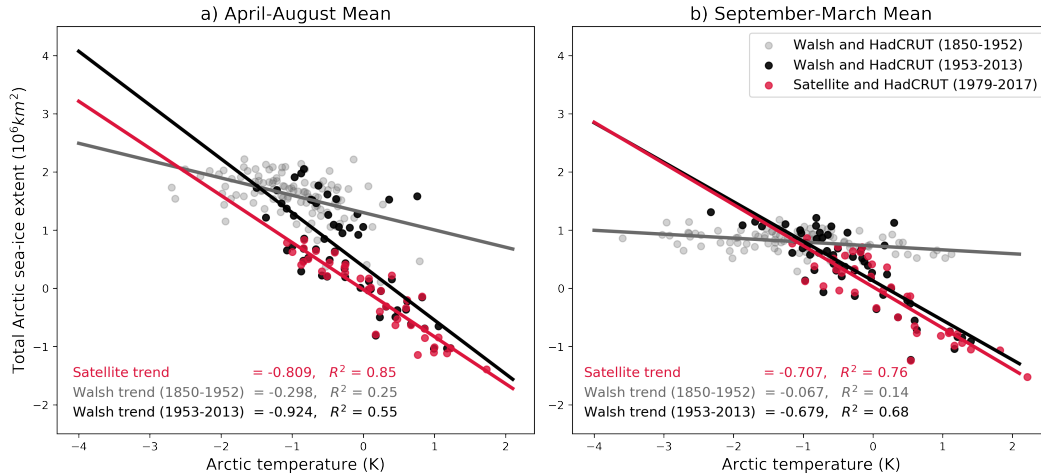


**Figure 1.** Arctic SAT (averaged north of  $65^{\circ}N$ , derived from HadCRUT) and total SIE in both the satellite data between 1979-2017 (in red) and the Walsh et al. (2017) data set between 1850 to 1952 (in gray) and 1953 to 2013 (in black). Anomalies are relative to 1979-2013.

111 not support this hypothesis. A second hypothesis is that the reduced sensitivity of sea  
 112 ice to temperature may simply be due to the fact that there are significantly fewer obser-  
 113 vations available to the Walsh et al. (2017) analysis prior to 1953 (as illustrated in  
 114 Supporting Information Figure S1).

115 The fidelity of sea-ice reconstructions has broader implications, as they are used  
 116 for boundary conditions in reanalysis products. The widely-used sea surface tempera-  
 117 ture and sea ice concentration HadISST2 product (Titchner & Rayner, 2014) incorpo-  
 118 rates an earlier version of the Walsh et al. (2017) sea-ice reconstruction (Walsh & Chap-  
 119 man, 2001), which is based largely on climatology for the first half of the 20th century.  
 120 Atmospheric reanalysis during the 20th century such as ERA-20C (Poli et al., 2016) com-  
 121 monly use HadISST2 as a boundary condition. Figure 2 shows temperature trends in  
 122 ERA-20C and the station-based HadCRUT (which uses no infill or interpolation). While  
 123 HadCRUT shows the large magnitudes and spatial extent of SAT trends during the ETCW,  
 124 in some locations comparable to the that during the recent satellite-era warming, ERA-  
 125 20C shows minimal trends across the Arctic. The NOAA/CIRES 20th Century reanal-  
 126 ysis (Compo et al., 2011) shows even larger biases than ERA-20C (see Supporting In-  
 127 formation Figure S2).

128 We postulate that these atmospheric reanalysis biases in simulating the ETCW are  
 129 strongly influenced by the small inter-annual sea-ice variability in Walsh and Chapman  
 130 (2001) that serve as boundary conditions. This hypothesis is consistent with Semenov  
 131 and Latif (2012), who find that the ETCW cannot be simulated with an atmospheric  
 132 model forced with HadISST1.1 (Rayner, 2003) boundary conditions, which show little  
 133 sea-ice variability prior to 1950. Thus improving sea-ice reconstructions has broad im-  
 134 plications, especially for studying high latitude climate variability.

135 To this end, we exploit the linear relationship between SAT and Arctic SIE evi-  
 136 dent in Figure 1 and in the literature (Mahlstein & Knutti, 2012) to reconstruct sea ice  
 137 using a DA approach. Other approaches have exploited this relationship to reconstruct  
 138 sea ice in the 20th century using linear regression models. For example, Connolly et al.  
 139 (2017) use pre-satellite temperature trends to re-calibrate sea-ice data sources from three  
 140 regions in the Arctic and find that sea ice retreated after the 1910s and advanced after  
 141 the mid 1940s, though the magnitude of these changes are small relative to the satellite

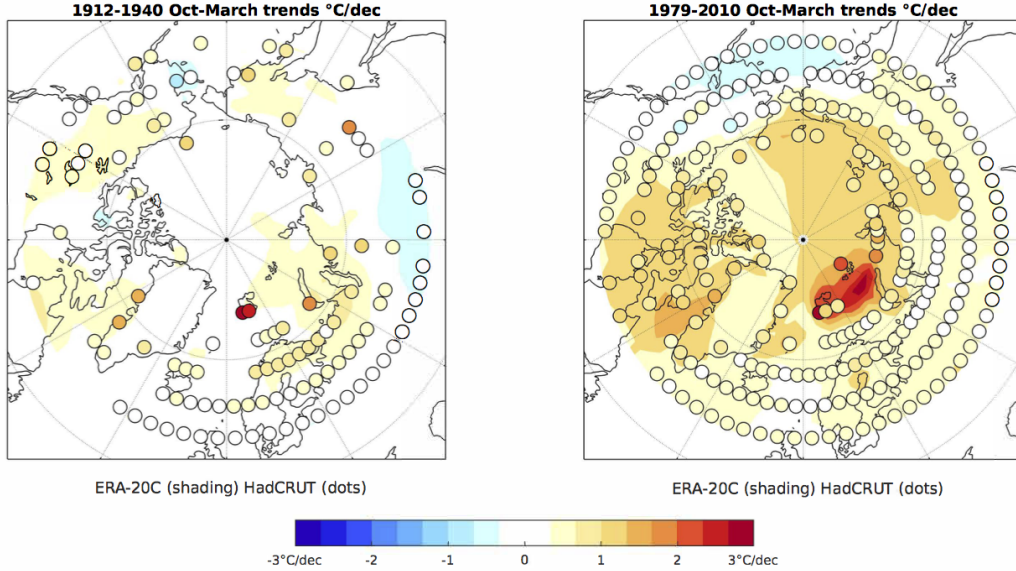


**Figure 2.** Temperature trends from ERA-20C are shown in shading and that from HadCRUT overlaid as shaded dots for both the early 20th century (1912–1940, left) and satellite era (1979–2010, right).

142 era. Alekseev et al. (2016) use the relationship between summer SAT and SIE to recon-  
 143 struct total Arctic SIE with a linear regression model, finding a decline of total Arctic  
 144 SIE of  $\sim 2 \times 10^6$  km<sup>2</sup> between 1900–1940 followed by a recovery that peaked around 1970.  
 145 The main benefit of the DA approach described here is the use of high quality 2 mair  
 146 temperature observations with a robust framework for uncertainty quantification (see  
 147 Section 3). Moreover, the results provide fully-gridded, spatially consistent climate fields  
 148 that can be used as boundary conditions for models and to probe the dynamics associ-  
 149 ated with sea-ice variability.

### 150 3 A new sea-ice reconstruction using data assimilation

#### 151 3.1 Data Assimilation approach

152 DA aims to optimally combine spatial data with noisy and sparse observations, re-  
 153 sulting in a better estimate of climate fields. Generally, DA updates a prior estimate,  
 154 an initial ‘best guess’, of the climate state with new information from observations. DA  
 155 allows point-wise observations of temperature to influence broader spatial regions of other  
 156 climate variables, like sea ice, based on the covariance relationships derived from the prior.  
 157 The prior estimate and observations are weighted based on their relative uncertainty, yield-  
 158 ing continuous fields.

159 To reconstruct Arctic sea ice we use an offline (Oke et al., 2002) ensemble Kalman  
 160 filter approach to combine Last Millennium climate model simulations (Schmidt et al.,  
 161 2011; Taylor et al., 2012) with temperature observations. The prior,  $\mathbf{x}^b$ , is an ensemble  
 162 of 200 random years drawn from these Last Millennium simulations (more details are  
 163 provided in Section 3.2). The update to this prior estimate uses annually averaged tem-  
 164 perature observations,  $\mathbf{y}$ , weighted as  $\mathbf{y} - \mathbf{H}\mathbf{x}^b$  (the ‘innovation’),

$$\mathbf{x}^a = \mathbf{x}^b + \mathbf{K}(\mathbf{y} - \mathbf{H}\mathbf{x}^b). \quad (1)$$

165 The innovation weight that results in the analysis,  $\mathbf{x}^a$ , is given by the Kalman gain,

$$\mathbf{K} = \mathbf{B}\mathbf{H}^T(\mathbf{H}\mathbf{B}\mathbf{H}^T + \mathbf{R})^{-1}, \quad (2)$$

166 where  $\mathbf{B}$  is the error covariance matrix of the prior,  $\mathbf{R}$  is the error covariance matrix of  
 167 the observations, and  $\mathbf{T}$  is the transpose operator. Matrix  $\mathbf{H}$  maps the prior to the ob-  
 168 servations by selecting grid-point data in the prior nearest to the observations. The Kalman  
 169 gain spreads the new information from temperature observations both spatially and to  
 170 other climate variables, weighted by the relative uncertainty of each. We sample tem-  
 171 perature observations from instrumental datasets every  $10^\circ$  latitude and longitude, cho-  
 172 sen to ensure the observation errors are uncorrelated and therefore  $\mathbf{R}$  is diagonal. This  
 173 assumption allows us to use serial observation processing, which assimilates observations  
 174 one at a time, simplifying implementation of spatial covariance localization as described  
 175 below.

176 To solve (1), we employ a square-root ensemble Kalman filter (Whitaker & Hamill,  
 177 2002), which updates the ensemble mean and the perturbations from the ensemble mean  
 178 separately. The Kalman gain used in the update equation for the ensemble perturbations  
 179 ( $\tilde{\mathbf{K}}$ ) is adjusted by a constant  $\alpha$  to yield the correct posterior covariance matrix. There-  
 180 fore,  $\tilde{\mathbf{K}} = \alpha\mathbf{K}$ , where, for a single observation,  $i$ ,

$$\alpha = \left( 1 + \sqrt{\frac{\mathbf{R}_{ii}}{\mathbf{H}\mathbf{B}\mathbf{H}^T_{ii} + \mathbf{R}_{ii}}} \right)^{-1}, \quad (3)$$

181 where  $ii$  denotes the matrix diagonal entry in the  $i$ th row and column.

182 As is standard practice in ensemble DA, we reduce the effect of spurious long-distance  
 183 covariances using covariance localization (e.g. Hamill et al. (2001)), applying the Gaspari-  
 184 Cohn fifth order polynomial function (Gaspari & Cohn, 1999) with a localization radius  
 185 (the distance from observations set to zero influence) of 15,000 km.

186 Kalman filter methods rely on the covariance in the prior ensemble between tem-  
 187 perature and the variables of interest (here, sea ice concentration, SIC). Climate mod-  
 188 els tend to underestimate the sensitivity of Arctic sea-ice loss to temperature (Rosenblum  
 189 & Eisenman, 2017; Winton, 2011; Stroeve et al., 2007). To address this low-sensitivity  
 190 bias, we inflate the sea-ice perturbations from the prior ensemble-means for the simu-  
 191 lations used here, MPI and CCSM4 Last Millennium simulations (see Section 3.2), by  
 192 a factor of 1.8 and 2.6, respectively. The inflation factors are determined empirically by  
 193 goodness of fit to the observed sea-ice trend during the satellite era. Sensitivity of the  
 194 results to the localization radius and inflation factor is explored below and in the Sup-  
 195 porting Information (see figures S4 and S5).

196 Since the Kalman filter method assumes Gaussian distributions, and SIC has a range  
 197 of 0–100%, unphysical values of  $\mathbf{x}^a$  outside this range may occur. Therefore, SIC values  
 198 outside the lower and upper end of this range are adjusted to 0% and 100%, respectively.

### 199 3.2 Data Sources

200 A 200-member prior ensemble of both SAT and SIC fields are randomly drawn from  
 201 fully forced Last Millennium model simulations spanning the years 850–1849 CE (Schmidt  
 202 et al., 2011; Taylor et al., 2012) (tests with a 1000-member prior ensemble revealed small  
 203 differences in Arctic SIE reconstructions,  $R^2 > 0.97$ , from the less computationally ex-  
 204 pensive case with a 200 member prior ensemble). Results using the Community Climate  
 205 System Model version 4 (CCSM4, Last Millennium simulation (Landrum et al., 2013))  
 206 and Max Planck Institute for Meteorology (MPI-ESM-P, Last Millennium simulation (Taylor  
 207 et al., 2012)) models are used to determine the sensitivity of the sea-ice reconstructions  
 208 to climate-model prior, and thus the sensitivity of the results to model physics and sea-  
 209 ice–temperature covariance structure. All model output is regridded to a  $\sim 2^\circ \times 2^\circ$  grid.

210 Sensitivity to the choice of instrumental temperature record is tested using three  
 211 different products: HadCRUT, Berkeley Earth (BE, (Rohde et al., 2013)), and NASA  
 212 Goddard Institute for Space Studies (GISTEMP, (Hansen et al., 2010)). An estimate of  
 213 the uncertainty in these observations is required when using an ensemble Kalman filter  
 214 approach (i.e.,  $\mathbf{R}$  in Equations 2 and 3), and HadCRUT is the only product that pro-  
 215 vides uncertainty estimates. Various ways of calculating  $\mathbf{R}$  were tested, (see Support-  
 216 ing Information), but in order to use all three products, and for simplicity, we use an un-  
 217 certainty estimate of  $0.4 \text{ K}^2$ , which is the area-weighted mean error variance provided  
 218 by HadCRUT.

#### 219 4 Arctic sea-ice reconstructions

220 We first reconstruct annual Arctic SIC for 1850–2018 by assimilating HadCRUT  
 221 SAT with a prior ensemble drawn from the MPI Last Millennium simulation. Figure 3  
 222 shows annual Arctic SIE (total area with SIC greater than or equal to 15%) derived from  
 223 the gridded SIC reconstructions. The timeseries is the mean of 5 independent iterations  
 224 that each use a different 200 member prior ensemble, in order to take into account the  
 225 uncertainty due to sampling error. Our reconstruction compares well with satellite ob-  
 226 servations (Figure 3) with  $R^2$  value of 0.89, detrended  $R^2$  value of 0.43, and coefficient  
 227 of efficiency (see Supporting Information Equation 1) of 0.89 between 1979–2017. The  
 228 trend during this period is well captured in the reconstructions with a value of  $-0.052 \pm 0.012 \times 10^6 \text{ km}^2/\text{year}$   
 229 compared to  $-0.055 \times 10^6 \text{ km}^2/\text{year}$  in satellite observations. Inter-annual variability is overestimated,  
 230 with a detrended standard deviation of  $0.21 \times 10^6 \text{ km}^2$  in the satellite observations and  $0.28 \times 10^6 \text{ km}^2$   
 231 in the reconstruction during 1979–2017.  
 232

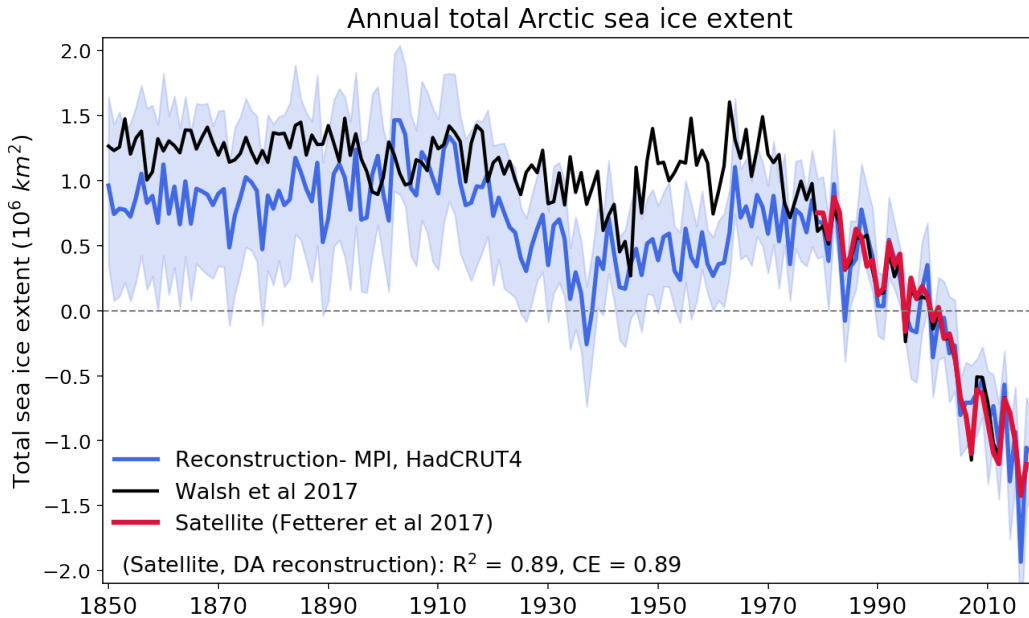


**Figure 3.** Reconstructed Arctic SIE from DA (blue), Walsh et al. (2017) (black), and satellite observations (red). For our reconstructions annually averaged HadCRUT temperature data was assimilated with a prior ensemble drawn from the MPI Last Millennium simulation. Anomalies are centered about 1979–2013.

233 The most notable feature of our reconstruction before the satellite era is the SIE  
 234 decline during the ETCW, with a total loss of about  $1.25 \times 10^6 \text{ km}^2$  between 1910–1940  
 235 compared to  $\sim 2.0 \times 10^6 \text{ km}^2$  lost between 1979–2017 in satellite observations. Between  
 236 1930–1950, our reconstruction also shows  $\sim 0.5 \times 10^6 \text{ km}^2$  less SIE than in the Walsh et  
 237 al. (2017) SIE record (see Figure 3), and the ETCW minimum occurs approximately eight  
 238 years earlier than in Walsh et al. (2017). Between 1850–1900 our reconstruction shows  
 239 a slow increase in SIE, reaching a maximum just after 1900, as opposed to the Walsh et  
 240 al. (2017) record which shows maximum SIE in the 1960s. Overall, prior to the satel-  
 241 lite era our reconstruction shows greater decadal variability compared to the Walsh et  
 242 al. (2017) record, which has relatively constant Arctic SIE between 1850–1970. Prior to  
 243 the satellite era (1850–1979) our reconstruction has a time-series standard deviation of  
 244  $310,000 \text{ km}^2$  whereas the Walsh et al. (2017) record has standard deviation of  $220,000$   
 245  $\text{km}^2$ . Though our reconstructions are annually resolved, they generally agree with the  
 246 summer reconstructions of Arctic SIE in Alekseev et al. (2016).

#### 247 4.1 Trends and variability

248 Next, we investigate the magnitude and significance of Arctic SIE trends during  
 249 the ETCW relative to the satellite era. In our reconstructions, the SIE decline in the ETCW  
 250 is shorter lived ( $\sim 25$ – $30$  years) than that in the satellite era ( $\sim 40$  years), thus we inves-  
 251 tigate the distribution of 25-year trends for both the satellite era and ETCW.

252 Figure 4 shows the distribution of trends calculated for each ensemble member (from  
 253 reconstructions using both MPI and CCSM4 model priors) for all possible 25-year seg-  
 254 ments during the satellite era (1979–2017) and the ETCW (1910–1940). The distribu-  
 255 tion of all 25-year trends between 1979–2017 for both Walsh et al. (2017) and satellite  
 256 observations are also shown as boxplots below the distributions. For the Walsh et al. (2017)  
 257 record, ETCW trends were calculated between 1918–1948 and are also shown as a box-  
 258 plot (we use a later window for a fair comparison since the minimum SIE occurred 8 years  
 259 later in Walsh et al. (2017)). The median 25-year trend found in the Walsh et al. (2017)  
 260 record during the ETCW of  $-0.18 \times 10^6 \text{ km}^2/\text{year}$  falls at the 98th and 99th percentiles  
 261 of the MPI and CCSM4 model prior reconstructions, respectively. We note that our re-  
 262 constructions slightly underestimate the mean 25-year trend in the satellite era. How-  
 263 ever, when comparing these two time periods in our reconstructions, the satellite era trends  
 264 are  $\sim 33$ – $38\%$  greater than the ETCW trends.

#### 265 4.2 Sensitivity of results

266 Our reconstruction of SIE depends on the gridded temperature product assimilated  
 267 (and associated errors), on the climate model prior, and on sample-error mediation in  
 268 the DA (localization length scale and ensemble variance inflation factor). A range of choices  
 269 for these aspects have been tested, with details provided in the Supporting Information.  
 270 Overall we find that the choice of observational dataset and model prior make little dif-  
 271 ference to pan-Arctic indices (see Figure S3 in Supporting Information), but that vari-  
 272 ance inflation and spatial localization have a larger affect.

273 With an offline DA approach, all temporal variability in the reconstruction comes  
 274 from the observations. Thus, increasing the localization radius and the ensemble vari-  
 275 ance inflation of sea ice relative to temperature, both increase the influence of temper-  
 276 ature observations, which is realized as larger temporal variability (Figure S4 and S5 in  
 277 Supporting Information). The results indicate a trade-off between capturing decadal vari-  
 278 ability versus inter-annual variability. For the MPI prior assimilated with HadCRUT tem-  
 279 perature, a localization length scale of 15,000 km leads to the best reconstructed trend  
 280 for nearly all inflation factors, so we chose to use this localization length scale. Given  
 281 a localization length scale of 15,000 km, the skill metrics are best for an inflation fac-  
 282 tor of 1.8. For a prior drawn from the CCSM4 Last Millennium simulation and HadCRUT

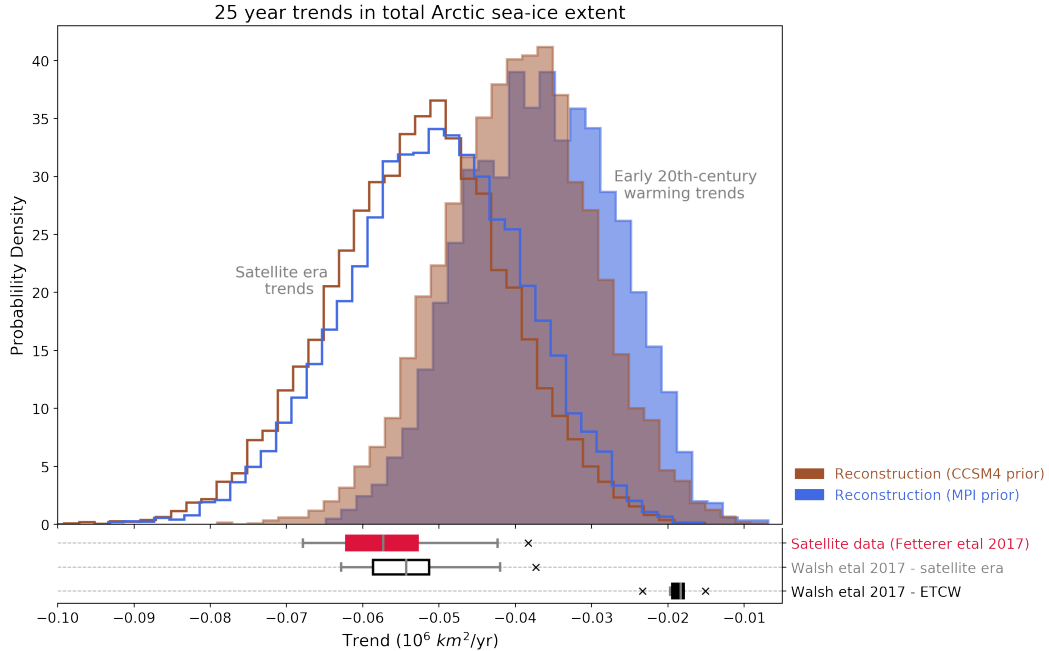


**Figure 4.** The distribution of all possible 25-year trends in Arctic SIE during the satellite era (1979–2017) and ETCW (1910–1940) for 5 prior iterations, each containing 200 ensemble members. The probability density functions show reconstructed SIE trends using MPI as the model prior (blue) and CCSM4 (brown). Below the histograms, the spread of trends calculated in the Walsh et al. (2017) record (black) and satellite observations (red) are displayed as box plots. The ETCW for the Walsh et al. (2017) record was calculated between 1918–1948.

283 observations, the same localization length scale of 15,000 km was used and an inflation  
 284 factor of 2.6 gave the best skill scores. Overall, these experiments show that a range of  
 285 values of localization and ensemble inflation result in skillful reconstructions relative to  
 286 satellite observations, and similar reconstructions of sea ice for earlier time periods.

287 **5 Conclusions**

288 The relationship between SIE and SAT is linear during the satellite era in obser-  
 289 vations, but we find that this relationship is much weaker or even absent in the Walsh  
 290 et al. (2017) record of SIE prior to the 1950s. This lower sensitivity of SIE to SAT in  
 291 the Walsh et al. (2017) record is plausibly due to a lack of high quality sea-ice obser-  
 292 vations, especially during fall and winter and prior to 1953. We have also found that 20th  
 293 century atmospheric reanalysis underestimate the magnitude of the ETCW (1910-1940)  
 294 in the Arctic. Since previous versions of the Walsh et al. (2017) dataset are used as bound-  
 295 ary conditions for 20th-century atmospheric reanalysis, we speculate that the low vari-  
 296 ability of SIE in Walsh et al. (2017) could be a reason atmospheric reanalysis do not fully  
 297 capture the ETCW, but leave exploration of this hypothesis to future work.

298 We exploit the relationship between SAT and SIC using an ensemble Kalman fil-  
 299 ter data assimilation approach to produce a new sea-ice reconstruction. This method op-  
 300 timally combines temperature observations and model data from Last Millennium simu-  
 301 lations to yield skillful Arctic sea-ice reconstructions with annual resolution. Validat-  
 302 ion against satellite observations yields an  $R^2$ -value of 0.89 and coefficient of efficiency  
 303 of 0.89. Prior to the satellite era, our reconstructions show Arctic SIE loss of  $\sim 1.25 \times$

304  $10^6$  km<sup>2</sup> during the ETCW, which is greater than the ETCW loss of  $\sim 0.75\text{--}1.0 \times 10^6$   
 305 km<sup>2</sup> estimated in Walsh et al. (2017), yet smaller than the SIE loss during the satellite  
 306 era of  $\sim 2.0 \times 10^6$  km<sup>2</sup>. The reconstructed 25-year trends of SIE indicate that the rate  
 307 of sea-ice loss during the ETCW was about  $\sim 33\text{--}38\%$  smaller than the 25-year trends  
 308 during the satellite era.

309 Overall, these reconstructions show more inter-annual variability in SIE than in Walsh  
 310 et al. (2017) during the Instrumental Era with standard deviation  $\sim 40\%$  ( $\sim 90,000$  km<sup>2</sup>)  
 311 greater between 1850–1979, a significant part due to the ETCW. The ETCW has been  
 312 ascribed to a combination of anthropogenic forcing and strong natural variability (Fyfe  
 313 et al., 2013; Delworth, 2000; Wood & Overland, 2009; Beitsch et al., 2014). Here we find  
 314 that during the satellite era, Arctic sea-ice loss was larger and longer lasting than dur-  
 315 ing the ETCW, which implies that the current declines likely necessitate external an-  
 316 thropogenic forcing, as previous results have shown (Ding et al., 2017; Kay et al., 2011;  
 317 Notz & Marotzke, 2012). Future work will extend this approach to reconstructing sea-  
 318 sonal variability and sea-ice thickness to further our understanding of sea ice during the  
 319 Instrumental era.

## 320 Acknowledgments

321 The data for these reconstructions will be uploaded to Zenodo upon acceptance.  
 322 The authors thank Cecilia Bitz and David Battisti for comments and ideas leading to  
 323 this project. MKB thanks Luke Parsons for insights into comparing trends and for test-  
 324 ing localization and inflation; Robert Tardif for contribution to development of the DA  
 325 code; Andre Perkins for software debugging help; Jessica Badgeley for productive dis-  
 326 cussions and support; and Robert Brennan for editing help. MKB was supported by the  
 327 NSF GRFP program. GH was supported by NSF award AGS-1602223 and NOAA award  
 328 NA18OAR4310422. EBW was supported by NOAA MAPP grant NA18OAR4310274.

## 329 References

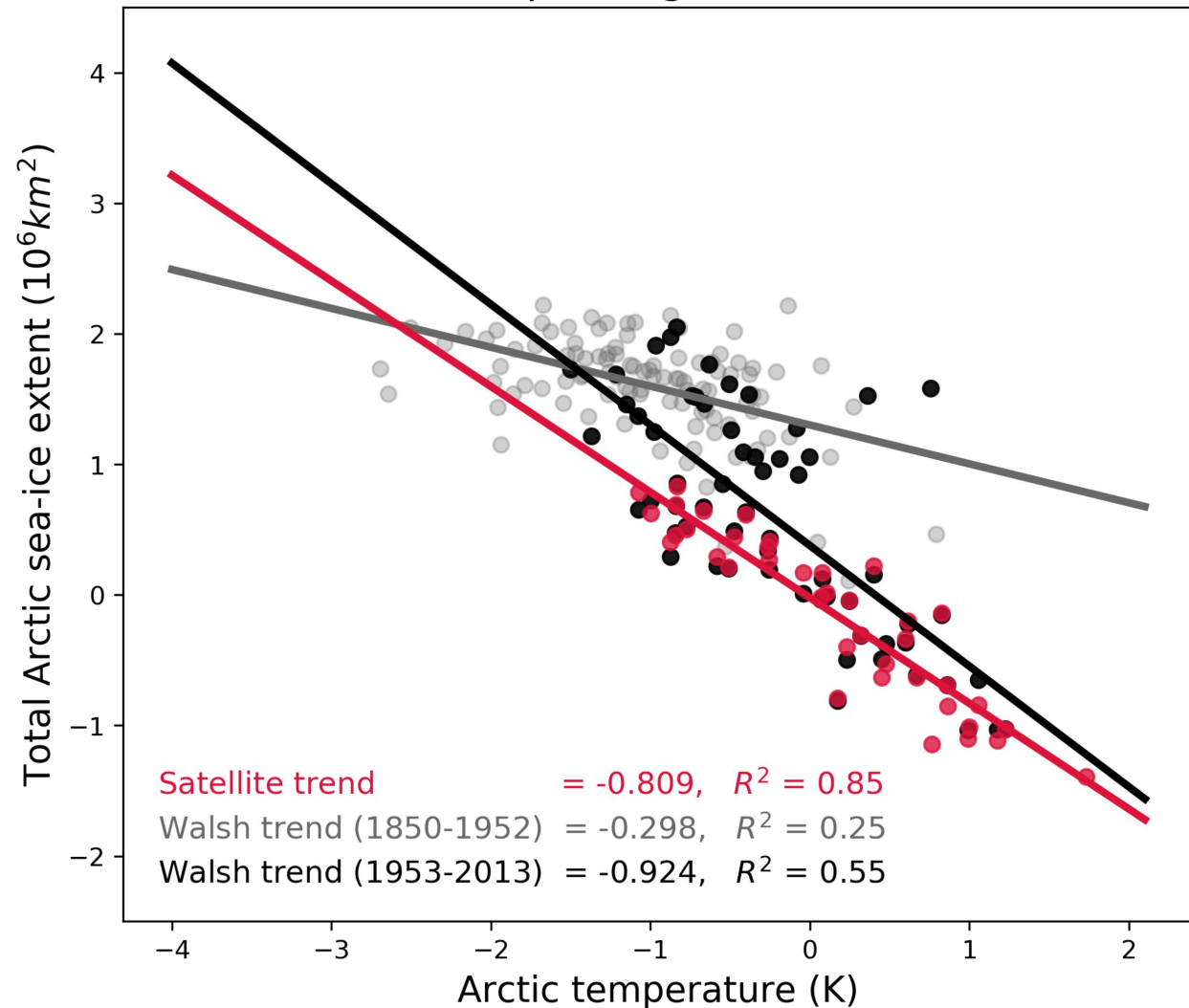
- 330 Alekseev, G., Glok, N., & Smirnov, A. (2016). On assessment of the relationship be-  
 331 tween changes of sea ice extent and climate in the Arctic. *International Jour-*  
 332 *nal of Climatology*, *36*(9), 3407–3412. doi: 10.1002/joc.4550
- 333 Armour, K. C., Eisenman, I., Blanchard-Wrigglesworth, E., McCusker, K. E., &  
 334 Bitz, C. M. (2011, aug). The reversibility of sea ice loss in a state-of-the-  
 335 art climate model. *Geophysical Research Letters*, *38*(16), n/a–n/a. doi:  
 336 10.1029/2011GL048739
- 337 Beitsch, A., Jungclaus, J. H., & Zanchettin, D. (2014, oct). Patterns of decadal-scale  
 338 Arctic warming events in simulated climate. *Climate Dynamics*, *43*(7-8), 1773–  
 339 1789. doi: 10.1007/s00382-013-2004-5
- 340 Compo, G. P., Whitaker, J. S., Sardeshmukh, P. D., Matsui, N., Allan, R. J., Yin,  
 341 X., . . . Worley, S. J. (2011, jan). The Twentieth Century Reanalysis Project.  
 342 *Quarterly Journal of the Royal Meteorological Society*, *137*(654), 1–28. doi:  
 343 10.1002/qj.776
- 344 Connolly, R., Connolly, M., & Soon, W. (2017). Re-calibration of Arctic sea ice  
 345 extent datasets using Arctic surface air temperature records. *Hydrological Sci-*  
 346 *ences Journal*, *62*(8), 1317–1340. doi: 10.1080/02626667.2017.1324974
- 347 Delworth, T. L. (2000, mar). Simulation of Early 20th Century Global Warming.  
 348 *Science*, *287*(5461), 2246–2250. doi: 10.1126/science.287.5461.2246
- 349 Ding, Q., Schweiger, A., L’Heureux, M., Battisti, D. S., Po-Chedley, S., Johnson,  
 350 N. C., . . . Steig, E. J. (2017, apr). Influence of high-latitude atmospheric cir-  
 351 culation changes on summertime Arctic sea ice. *Nature Climate Change*, *7*(4),  
 352 289–295. doi: 10.1038/nclimate3241
- 353 England, M., Jahn, A., & Polvani, L. (2019). Nonuniform contribution of internal

- 354 variability to recent Arctic sea ice loss. *Journal of Climate*, *32*(13), 4039–4053.  
355 doi: 10.1175/JCLI-D-18-0864.1
- 356 Fetterer, F., Knowles, K., Meier, W. N., Savoie, M., & Windnagel, A. K. (2017). Sea  
357 Ice Index, Version 3. *NSIDC: National Snow and Ice Data Center, Boulder,*  
358 *Colorado USA*. doi: 10.7265/N5K072F8
- 359 Fyfe, J. C., von Salzen, K., Gillett, N. P., Arora, V. K., Flato, G. M., & McConnell,  
360 J. R. (2013, dec). One hundred years of Arctic surface temperature variation  
361 due to anthropogenic influence. *Scientific Reports*, *3*(1), 2645. doi:  
362 10.1038/srep02645
- 363 Gaspari, G., & Cohn, S. E. (1999, jan). Construction of correlation functions in two  
364 and three dimensions. *Quarterly Journal of the Royal Meteorological Society*,  
365 *125*(554), 723–757. doi: 10.1256/smsqj.55416
- 366 Gregory, J. M., Stott, P. A., Cresswell, D. J., Rayner, N. A., Gordon, C., & Sexton,  
367 D. M. H. (2002, dec). Recent and future changes in Arctic sea ice simulated by  
368 the HadCM3 AOGCM. *Geophysical Research Letters*, *29*(24), 28–1–28–4. doi:  
369 10.1029/2001GL014575
- 370 Hamill, T. M., Whitaker, J. S., & Snyder, C. (2001, nov). Distance-Dependent  
371 Filtering of Background Error Covariance Estimates in an Ensemble  
372 Kalman Filter. *Monthly Weather Review*, *129*(11), 2776–2790. doi:  
373 10.1175/1520-0493(2001)129<2776:DDFOBE>2.0.CO;2
- 374 Hansen, J., Ruedy, R., Sato, M., & Lo, K. (2010, dec). GLOBAL SURFACE TEM-  
375 PERATURE CHANGE. *Reviews of Geophysics*, *48*(4), RG4004. doi: 10.1029/  
376 2010RG000345
- 377 Hegerl, G. C., Brönnimann, S., Schurer, A., & Cowan, T. (2018, jul). The early  
378 20th century warming: Anomalies, causes, and consequences. *Wiley Interdisci-*  
379 *plinary Reviews: Climate Change*, *9*(4), e522. doi: 10.1002/wcc.522
- 380 Kay, J. E., Holland, M. M., & Jahn, A. (2011, aug). Inter-annual to multi-decadal  
381 Arctic sea ice extent trends in a warming world. *Geophysical Research Letters*,  
382 *38*(15), 2–7. doi: 10.1029/2011GL048008
- 383 Landrum, L., Otto-Bliesner, B. L., Wahl, E. R., Conley, A., Lawrence, P. J.,  
384 Rosenbloom, N., & Teng, H. (2013, feb). Last Millennium Climate and  
385 Its Variability in CCSM4. *Journal of Climate*, *26*(4), 1085–1111. doi:  
386 10.1175/JCLI-D-11-00326.1
- 387 Mahlstein, I., & Knutti, R. (2012, mar). September Arctic sea ice predicted to disap-  
388 pear near 2C global warming above present. *Journal of Geophysical Research:*  
389 *Atmospheres*, *117*(D6), n/a–n/a. doi: 10.1029/2011JD016709
- 390 Meier, W. N., Hovelsrud, G. K., van Oort, B. E., Key, J. R., Kovacs, K. M., Michel,  
391 C., ... Reist, J. D. (2014, sep). Arctic sea ice in transformation: A review of  
392 recent observed changes and impacts on biology and human activity. *Reviews*  
393 *of Geophysics*, *52*(3), 185–217. doi: 10.1002/2013RG000431
- 394 Morice, C. P., Kennedy, J. J., Rayner, N. A., & Jones, P. D. (2012, apr). Quantify-  
395 ing uncertainties in global and regional temperature change using an ensemble  
396 of observational estimates: The HadCRUT4 data set. *Journal of Geophysical*  
397 *Research: Atmospheres*, *117*(D8), n/a–n/a. doi: 10.1029/2011JD017187
- 398 Notz, D., & Marotzke, J. (2012, apr). Observations reveal external driver for Arctic  
399 sea-ice retreat. *Geophysical Research Letters*, *39*(8), n/a–n/a. doi: 10.1029/  
400 2012GL051094
- 401 Oke, P. R., Allen, J., Miller, R. N., Egbert, G. D., & Kosro, P. M. (2002). Assim-  
402 ilation of surface velocity data into a primitive equation coastal ocean model.  
403 *Journal of Geophysical Research*, *107*(C9), 3122. doi: 10.1029/2000JC000511
- 404 Olonscheck, D., Mauritsen, T., & Notz, D. (2019, jun). Arctic sea-ice variability is  
405 primarily driven by atmospheric temperature fluctuations. *Nature Geoscience*,  
406 *12*(6), 430–434. doi: 10.1038/s41561-019-0363-1
- 407 Overland, J. E., Spillane, M. C., Percival, D. B., Wang, M., & Mofjeld, H. O. (2004,  
408 sep). Seasonal and Regional Variation of Pan-Arctic Surface Air Temperature

- 409 over the Instrumental Record\*. *Journal of Climate*, 17(17), 3263–3282. doi: 10  
410 .1175/1520-0442(2004)017<3263:SARVOP>2.0.CO;2
- 411 Poli, P., Hersbach, H., Dee, D. P., Berrisford, P., Simmons, A. J., Vitart, F.,  
412 ... Fisher, M. (2016, jun). ERA-20C: An Atmospheric Reanalysis of  
413 the Twentieth Century. *Journal of Climate*, 29(11), 4083–4097. doi:  
414 10.1175/JCLI-D-15-0556.1
- 415 Rayner, N. A. (2003). Global analyses of sea surface temperature, sea ice, and night  
416 marine air temperature since the late nineteenth century. *Journal of Geophys-  
417 ical Research*, 108(D14), 4407. doi: 10.1029/2002JD002670
- 418 Rohde, R., Muller, R., Jacobsen, R., Perlmutter, S., & Mosher, S. (2013). Berke-  
419 ley Earth Temperature Averaging Process. *Geoinformatics & Geostatistics: An  
420 Overview*, 01(02). doi: 10.4172/2327-4581.1000103
- 421 Rosenblum, E., & Eisenman, I. (2017, aug). Sea Ice Trends in Climate Models Only  
422 Accurate in Runs with Biased Global Warming. *Journal of Climate*, 30(16),  
423 6265–6278. doi: 10.1175/JCLI-D-16-0455.1
- 424 Schmidt, G. A., Jungclaus, J. H., Ammann, C. M., Bard, E., Braconnot, P., Crow-  
425 ley, T. J., ... Vieira, L. E. A. (2011, jan). Climate forcing reconstructions for  
426 use in PMIP simulations of the last millennium (v1.0). *Geoscientific Model  
427 Development*, 4(1), 33–45. doi: 10.5194/gmd-4-33-2011
- 428 Semenov, V. A. (2007). Structure of temperature variability in the high latitudes of  
429 the Northern Hemisphere. *Izvestiya - Atmospheric and Ocean Physics*, 43(6),  
430 687–695. doi: 10.1134/S0001433807060023
- 431 Semenov, V. A., & Latif, M. (2012, nov). The early twentieth century warming and  
432 winter Arctic sea ice. *The Cryosphere*, 6(6), 1231–1237. doi: 10.5194/tc-6-1231  
433 -2012
- 434 Stroeve, J., Holland, M. M., Meier, W., Scambos, T., & Serreze, M. (2007, may).  
435 Arctic sea ice decline: Faster than forecast. *Geophysical Research Letters*,  
436 34(9), 1–5. doi: 10.1029/2007GL029703
- 437 Taylor, K. E., Stouffer, R. J., & Meehl, G. A. (2012). An Overview of CMIP5 and  
438 the Experiment Design. *American Meteorological Society*.
- 439 Titchner, H. A., & Rayner, N. A. (2014, mar). The Met Office Hadley Centre  
440 sea ice and sea surface temperature data set, version 2: 1. Sea ice concentra-  
441 tions. *Journal of Geophysical Research: Atmospheres*, 119(6), 2864–2889. doi:  
442 10.1002/2013JD020316
- 443 Walsh, J. E., & Chapman, W. L. (2001). 20Th-Century Sea-Ice Variations From Ob-  
444 servational Data. *Annals of Glaciology*, 33(1979), 444–448.
- 445 Walsh, J. E., Fetterer, F., Scott Stewart, J., & Chapman, W. L. (2017, jan). A  
446 database for depicting Arctic sea ice variations back to 1850. *Geographical Re-  
447 view*, 107(1), 89–107. doi: 10.1111/j.1931-0846.2016.12195.x
- 448 Whitaker, J. S., & Hamill, T. M. (2002). Ensemble Data Assimilation without Per-  
449 turbed Observations. *Monthly Weather Review*, 130(7), 1913–1924. doi: 10  
450 .1175/1520-0493(2002)130<1913:edawpo>2.0.co;2
- 451 Winton, M. (2011). Do climate models underestimate the sensitivity of Northern  
452 Hemisphere sea ice cover? *Journal of Climate*, 24(15), 3924–3934. doi: 10  
453 .1175/2011JCLI4146.1
- 454 Wood, K. R., & Overland, J. E. (2009). Early 20 th century Arctic warming in ret-  
455 rospect. *International Journal of Climatology*, 30(9), n/a–n/a. doi: 10.1002/  
456 joc.1973

Figure 1.

a) April-August Mean



b) September-March Mean

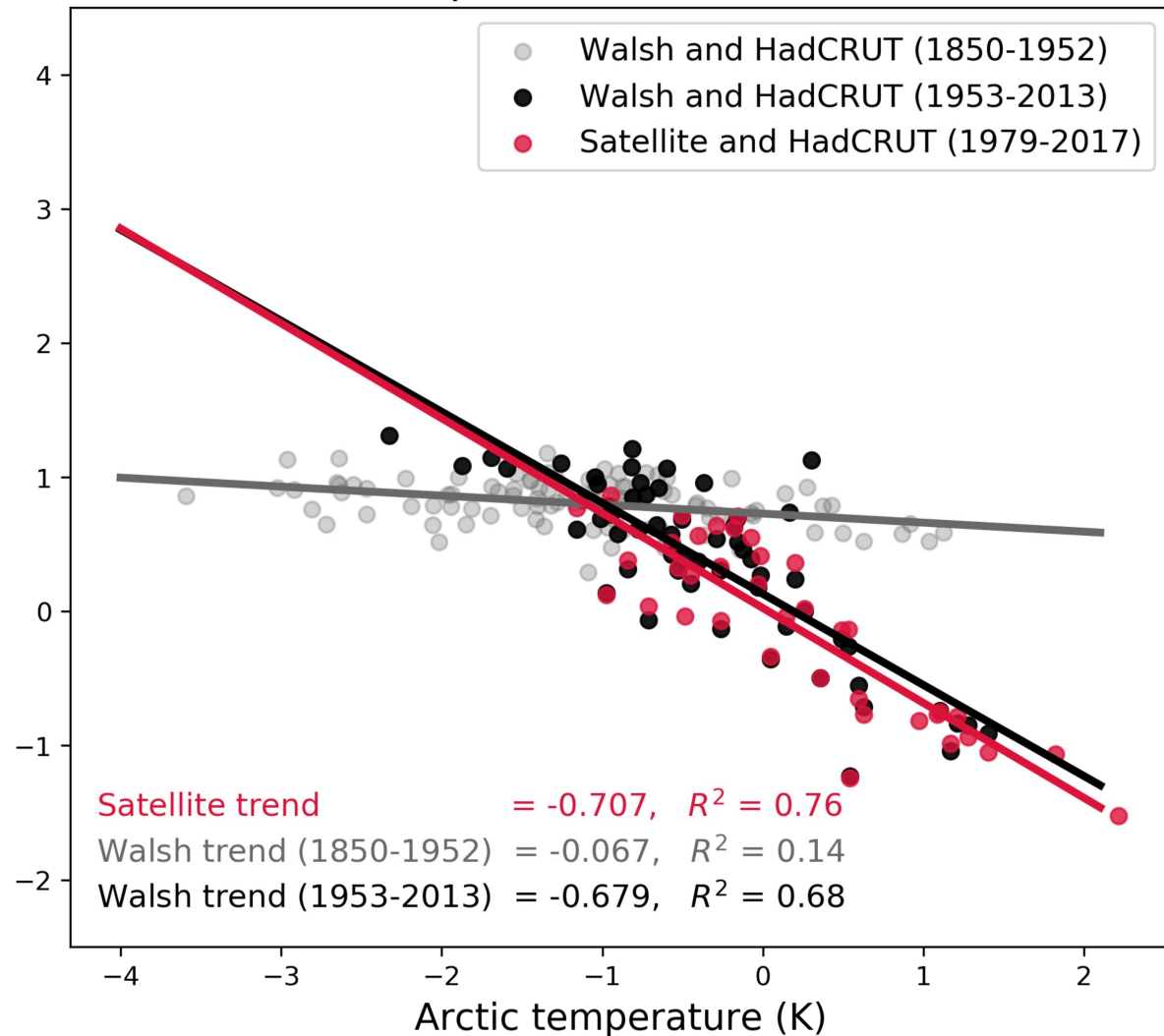
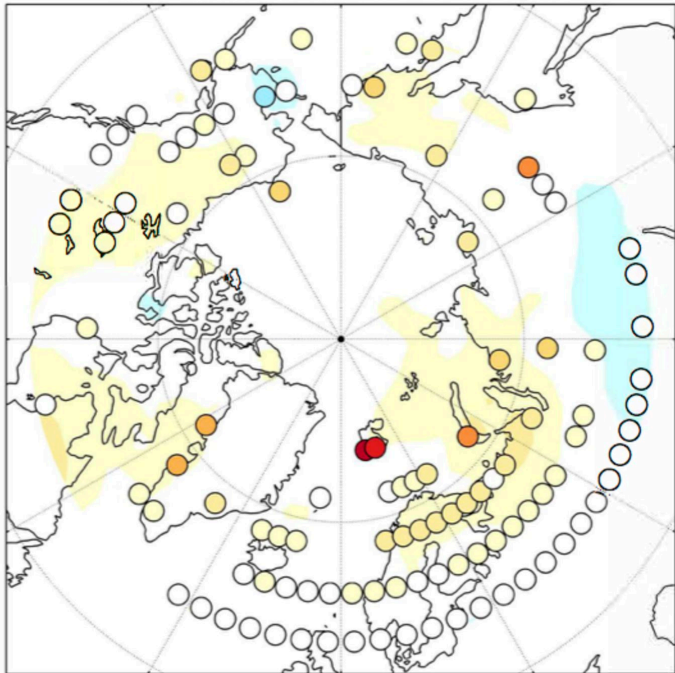


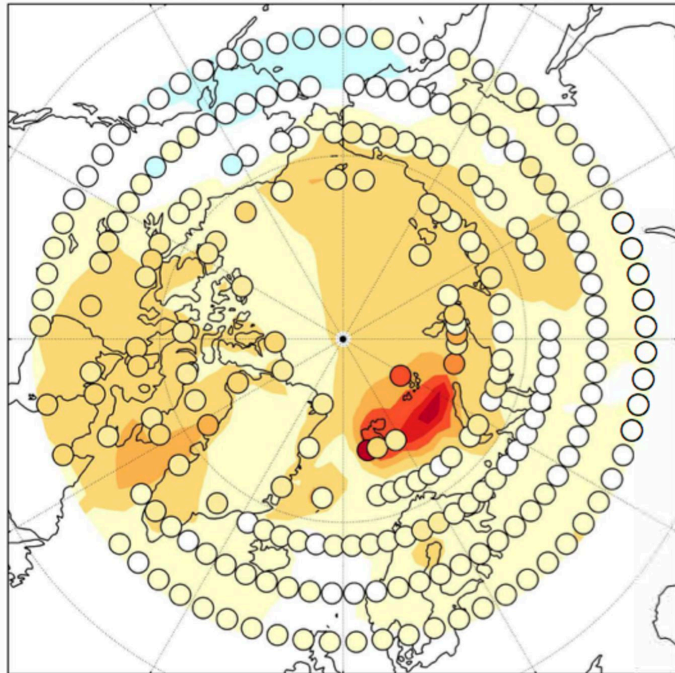
Figure 2.

1912-1940 Oct-March trends °C/dec



ERA-20C (shading) HadCRUT (dots)

1979-2010 Oct-March trends °C/dec



ERA-20C (shading) HadCRUT (dots)

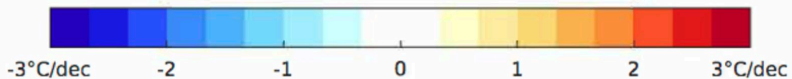
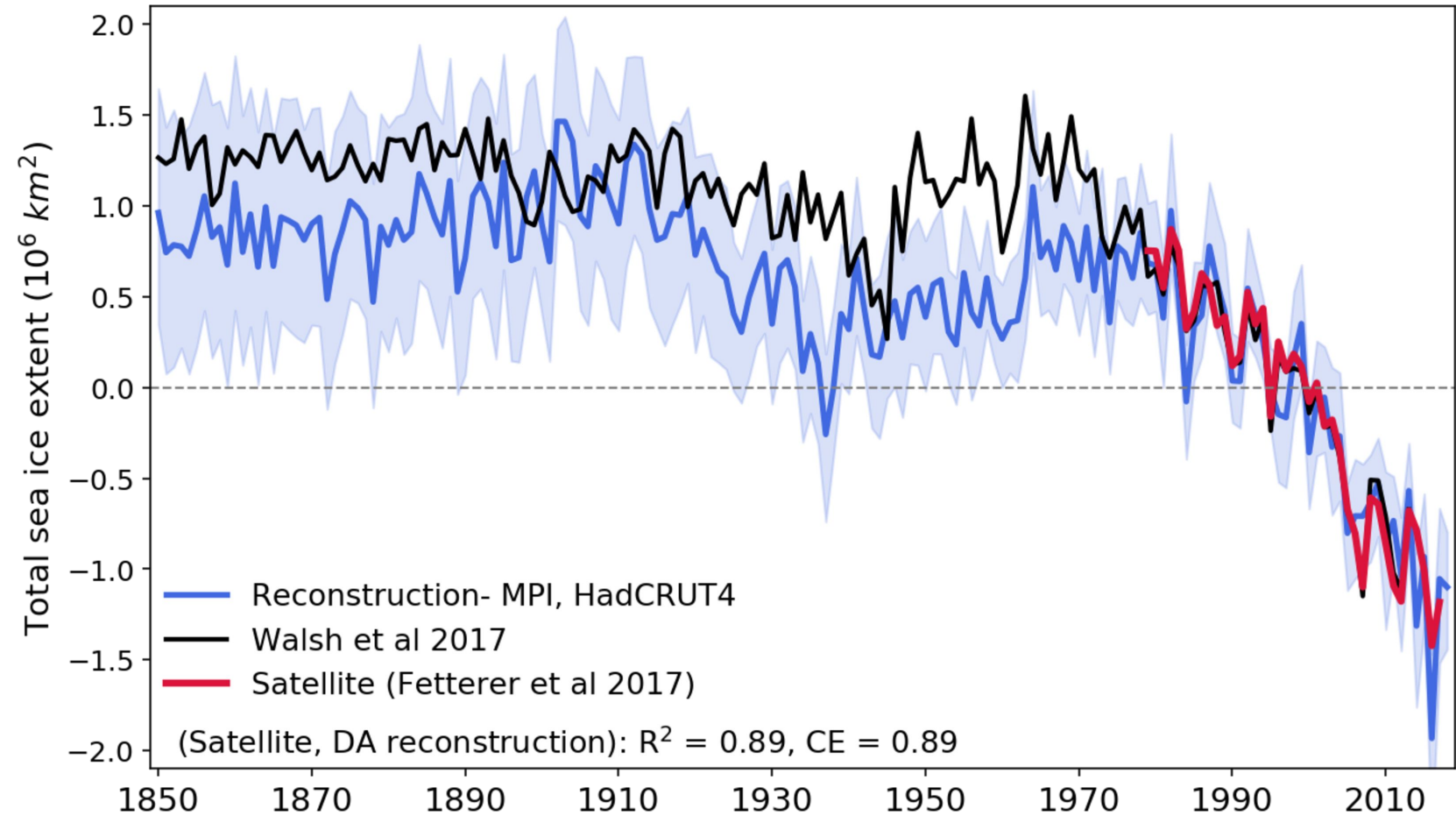


Figure 3.

# Annual total Arctic sea ice extent



**Figure 4.**

# 25 year trends in total Arctic sea-ice extent

